Endo *Progress in Earth and Planetary Science* (2016) 3:28
DOI 10.1186/s40645-016-0102-9

Progress in Earth and Planetary Science

RESEARCH ARTICLE Open Access

Simple stochastic cellular automaton model for starved beds and implications about formation of sand topographic features in terms of sand flux

Noritaka Endo

Abstract

A simple stochastic cellular automaton model is proposed for simulating bedload transport, especially for cases with a low transport rate and where available sediments are very sparse on substrates in a subaqueous system. Numerical simulations show that the bed type changes from sheet flow through sand patches to ripples as the amount of sand increases; this is consistent with observations in flume experiments and in the field. Without changes in external conditions, the sand flux calculated for a given amount of sand decreases over time as bedforms develop from a flat bed. This appears to be inconsistent with the general understanding that sand flux remains unchanged under the constant-fluid condition, but it is consistent with the previous experimental data. For areas of low sand abundance, the sand flux versus sand amount (flux–density relation) in the simulation shows a single peak with an abrupt decrease, followed by a long tail; this is very similar to the flux–density relation seen in automobile traffic flow. This pattern (the relation between segments of the curve and the corresponding bed states) suggests that sand sheets, sand patches, and sand ripples correspond respectively to the free-flow phase, congested phase, and jam phase of traffic flows. This implies that sand topographic features on starved beds are determined by the degree of interference between sand particles. Although the present study deals with simple cases only, this can provide a simplified but effective modeling of the more complicated sediment transport processes controlled by interference due to contact between grains, such as the pulsatory migration of grain-size bimodal mixtures with repetition of clustering and scattering.

Keywords: Stochastic cellar automaton, Bedload transport, Sand patches, Sand sheets, Sand ripples

Correspondence: wisteria@staff.kanazawa-u.ac.jp
Department of Earth Sciences, Graduate School of Natural Science & Technology, Kanazawa University, Kakuma-machi, Kanazawa, Ishikawa 920-1192, Japan

Introduction

Bedforms, including both subaerial and subaqueous ones, have been studied for more than half a century, mainly starting with the pioneering field observations of Bagnold (1941) and the laboratory studies of Allen (1968) and continuing to recent comprehensive experiments (e.g., Perillo et al. 2014). Theoretical studies also have been conducted, employing various approaches, such as linear and nonlinear stability analyses (e.g., Melo et al. 2012; Andreotti et al. 2012); first-principle calculations for fluids and/or grains (e.g., Wippermann and Gross 1986; Schwämmle and Herrmann 2003; Duran et al. 2014); simulations with simplified continuous models, such as a defect-crest line dynamics model (Werner and Kocurek 1999), a skeleton model (Niiya et al. 2010), and a single-dune-based particle model (Parteli and Herrmann 2003; Diniega et al. 2010); and simulations with various cellular automaton (CA) models (e.g., Nishimori and Ouchi 1993; Werner 1995; Momiji et al. 2000; Katsuki et al. 2005). Even with increased computing speeds, CA models of bedforms remain useful for complicated settings that are time consuming when other methods are used (Barchyn and Hugenholtz 2012; Barrio-Parra and Rodríguez-Santalla 2014; Rozier and Narteau 2014).

The transport of sand grains in water can be classified into four modes: sliding, rolling, saltation, and suspension (Allen 1982). Sliding and rolling grains remain in continuous contact with the bed, while suspended particles have little or no contact with the bed. Saltating grains jump over the bed in a series of low trajectories that are on the order of 10 to 20 particle diameters long and a few diameters high; thus, this is an intermediate mode between sliding and rolling and suspension. Reid and Frostick (1994) defined the bedload as the grains that move along the bed and that are essentially in contact with it at all times (i.e., including only sliding and rolling particles) and independently defined the saltation load; however, others (e.g., Allen 1982; Bridge and Demicco 2008) defined the bedload to include saltating grains in addition to sliding and rolling grains. Regardless of the definition of bedload, all researchers have pointed out that in subaqueous environments, sliding and rolling are most prevalent when the level of transport is low (low transport stage; Allen 1982; Reid and Frostick 1994; Bridge and Demicco 2008).

Allen (1982) pointed out that in air and water, transport processes differ due to the difference in viscosity and density of the medium. In the case of aeolian dunes, saltation is the most important mode (Bagnold 1941), whereas bedload transport is most important for subaqueous ripples (Allen 1968). Sand ripples can be generated by a shear stress that is just above the threshold for bedload transport (Bridge and Demicco 2008). In subaqueous environments, sliding and rolling are most prevalent at low transport stages (Allen 1982; Reid and Frostick 1994; Bridge and Demicco 2008), and therefore, instead of considering changes in saltation length, the subaqueous bedform at low transport stages should be explained by a model that considers grain movements that are in continuous contact with the bed. Although previous CA models for aeolian dunes have attributed the bedform generation to changes in the saltation length, in the present study, which employs a stochastic model, we consider changes of the migration speed of sand particles that are in continuous contact with the bed (i.e., sand that moves no faster than one cell per time step). Although there have been a few preliminary attempts to employ the CA model and explicitly include the continuous bed-contact load (e.g., Miyata and Iwasa 1997), the relation between sand flux and sand abundance was not considered.

Historically, most sedimentological and geomorphological studies of subaqueous beds have considered beds in which sand covered the entire substrate, i.e., sediment beds. It is known that on starved beds (nonerodible substrates with sparse sand), there occur topographic features that are different from those that occur on sediment beds, for example, sand patches. For starved beds, the relation between the sand flux and the topographic features has not been sufficiently studied. Although Betat et al. (2002) measured the bedload flux for sediment beds, there are few such studies, because it is difficult to measure the sand flux without disturbing the system; this is especially true for starved beds. Numerical simulations can provide useful information about the generation and transition of sand topographic features on starved beds, such as sand patches.

In this paper, we consider sparse sediments under relatively slow, unidirectional water flow; we present a CA model and discuss the relation between bed states and sand flux. We compare the results of our model with the results of a jam simulated by a traffic flow model. The jam-like transportation of sediments has been reported, such as sediments passing a meander bend of a channel with a pool (Kleinhans et al. 2002) and the pulsatory migration of sediment mixtures with grain-size bimodality (Iseya and Ikeda 1987). Following perturbations in the sediment supply, sparsely distributed sediments in a bedrock channel cause both negative and positive feedback to the incision rate (Finnegan et al. 2007). Although applications to such complicated natural phenomena are beyond the scope of this study, we note that the CA model is a potential tool for a deeper understanding of the dynamics of starved beds.

The purposes of the present study are as follows: (1) to propose a new CA model that includes the continuous bed-contact load in small-scale subaqueous beds with sparsely available sediments; (2) to compare the

results of our model to those of flume experiments to assess how well it models changes in topographic features with increasing levels of sand abundance, as well as temporal changes in the sand flux under constant conditions (this has not previously attracted much attention); and (3) to gain a better understanding of the dynamics of bed states by investigating the dependence of the sand flux on the abundance sand and topographic features; we do this by a comparison with other kinds of physical phenomena, such as traffic flow.

Methods/Experimental

CA model

CA models include the coarse graining of sand by considering clusters of sand grains (sand slabs) instead of individual particles. In CA models, the topographic height is taken to be the number of compiled slabs. The topographic height *h(i, j)* at site (*i*, *j*) in a two-dimensional field changes with time. Previous CA models for aeolian sand dunes used a phenomenological formulation of saltation; that is, it was not based on fluid motion. Although there is some variation in the formulations of saltation, the previous models determined situational-specific saltation distances, such as defining the jumping length as a function of the state of the sand bed.

Allen (1982) pointed out that the differences in air and water transport stemmed from differences in the viscosity and density of the medium. On subaqueous beds under relatively slow flows, the main transport mode of sand grains is rolling and sliding, for which bed contact is continuous (Allen 1982; Reid and Frostick 1994; Bridge and Demicco 2008). Therefore, instead of using the saltation length, low transport stages of subaqueous bedforms can be better explained by incorporating changes in the migration speed of grains in continuous contact with the bed. In the simulation used in the present study, the movement of particles was considered separately for two processes: transport due to fluid motion, with continuous bed contact; and avalanching due to gravity. For the remainder of this paper, we will use "bedload" to mean the continuous bed-contact load that is only due to the flow (not due to gravity). Other processes due to flow, such as saltation or suspension, will not be considered so that we can focus on subaqueous environments with low transport rates that form topographies such as sand patches. In the simulation, which process (bedload transport or avalanching) occurs is evaluated deterministically from the geomorphological state of the position. However, the movement of sand slabs due to bedload transport is a stochastic variable that expresses finite velocities for discrete positions; that is, slabs migrate according to a probability that represents the velocity (see below). The simulation ignores the inner structure of the flow, which becomes important when the flow is relatively fast and the bed roughness (bedforms) is large; for simplicity, we ignore the effects of strong erosional vortices and secondary flows.

Formulation of bedload transport

When simulating bedload transport in a CA model, sand slabs should be restricted to moving to the adjacent downstream cell, unlike the process for saltation. The topographic height is affected by bedload transport as follows:

$$h(i,j)\rightarrow h(i,j)-q_b \text{ and } h(i+1,j)\rightarrow h(i+1,j)+q_b, \quad (1)$$

where site $(i+1, j)$ is downstream of site (i, j), and q_b is the number of slabs that migrate during a single calculation step. Here, we consider bedload transport in only the direction of the flow; this is the positive x-direction of the two-dimensional (x, y) system.

If the bed is perfectly uniform, sand may be transported everywhere at a constant rate, but otherwise, the rate of sand migration depends on the location. We formulated a simple phenomenological rule for the probability of sand movement (surrogate of velocity) that does not require calculating the fluid motion. In each time step, a sand slab on the surface moves to the next downstream cell or remains at the same location, as determined stochastically; this probability corresponds to the velocity of the sand migration velocity (that is, a higher probability corresponds to a higher velocity), and this depends on the state of each site.

We made the following assumptions. Sand slabs on a stoss side move fastest at the local peak (state s1), and other sand slabs (for example, partway down the slope) slow down as the downstream gradient increases, due to the competing gravitational force. Sand slabs on lee slopes move more slowly than those on stoss slopes, because to some extent, the bedform shields the downstream flow. For a slab on a lee slope, the probability of movement depends on the extent of the shielding effect of the bedform; we assume that this depends on the gradient of the lee slope. When the slope of a lee side is less than a certain value (state s3), slabs can move as a bedload; otherwise, if the slope is greater than or equal to a threshold value (state s4), slabs are in a perfectly shielded area (shadow zone), in which the flow is not sufficient to convey sand as a bedload, and thus, the sand moves only by avalanching. From these assumptions, we obtain a simple formulation for the state-dependent (s1 to s4) probability, $B_{i,j}$, that the sand at site (i, j) will migrate by bedload transport to the nearest downstream cell:

$$B_{i,j} = \begin{cases} \alpha & \text{on a local peak, including a flat top (s1)} \\ \alpha/\,(h(i+1,\,j)-h(i,\,j)) & \text{midway along a stoss side (s2)} \\ \gamma\{\beta-\,(h(i-1,\,j)-h(i,\,j))\} & \text{on a lee slope, but not in a shadow zone (s3)} \\ 0 & \text{in a shadow zone (s4)}, \end{cases} \tag{2}$$

where α, β, and γ are positive constants. The second expression on the right-hand side shows that the difficulty of climbing a stoss slope depends on the gradient. The third expression on the right-hand side shows the extent to which the bedform reduces the flow, as a function of the gradient of the lee slope.

In Eq. (2), the condition of the local state (s1 to s4) is determined as follows. If $h_{i-1,j} \leqq h_{i,j}$, the site (i, j) is on a stoss slope or at a local peak. If it is also true that $h_{i+1,j} - h_{i,j} \leqq 0$, then the site is a peak or a flat top (s1); otherwise, it is somewhere along a stoss slope (s2), and the velocity is inversely proportional to the gradient. On the other hand, if $h_{i-1,j} > h_{i,j}$, the site (i, j) is on a lee slope. If it is also true that $h_{i-1,j} - h_{i,j} \leqq \beta$, then site (i, j) is not in a shadow zone (s3); otherwise, it is in a shadow zone (s4). Note that β is the threshold value for the shadow zone. The above determination of the site state for the bedload (s1 to s4) can be summarized as follows:

$$\begin{cases} \text{if } h_{i-1,j} \leqq h_{i,j} \text{ and } \begin{cases} \text{if } h_{i+1,j} - h_{i,j} \leqq 0 & : (s1) \\ \text{if } h_{i+1,j} - h_{i,j} > 0 & : (s2) \end{cases} \\ \text{if } h_{i-1,j} > h_{i,j} \text{ and } \begin{cases} \text{if } h_{i-1,j} - h_{i,j} \leqq \beta & : (s3) \\ \text{if } h_{i-1,j} - h_{i,j} > \beta & : (s4) \end{cases} \end{cases}. \tag{3}$$

Formulation of avalanching

Avalanching occurs as a result of gravity, and consequently, sand can be conveyed by avalanching in a shadow zone, even when bedload transport does not occur. Avalanching occurs when the lee slope is steeper than the angle of repose; the probability that avalanching occurs is unity, which implies deterministic and immediate movement. For avalanching in the streamwise direction at site (i, j), the topographic height at (i, j) develops as follows:

$$h(i,j) \rightarrow h(i,j) - q_a \text{ and } h(i+1,j) \rightarrow h(i+1,j) + q_a, \tag{4}$$

where q_a is the number of slabs that move by avalanching during one time step. According to flume experiments, avalanching does not occur on a stoss side; thus, we do not need to consider avalanching in the negative x-direction. Avalanching always occurs if the following condition is satisfied:

$$\{\text{downward slope}\} > A_r \text{ with the condition } (s4), \tag{5}$$

where A_r is a positive constant that represents the angle of repose, and the slope in the downstream (positive x-direction) is defined as

$$\{\text{downward slope}\} = h(i,j) - h(i+1,j). \tag{6}$$

Unlike with bedload transport, because of gravity, avalanching can also occur in the lateral direction:

$$h(i,j) \rightarrow h(i,j) - q_a \text{ and } \begin{cases} h(i,j+1) \rightarrow h(i,j+1) + q_a \\ \text{or } h(i,j-1) \rightarrow h(i,j-1) + q_a \end{cases}\!\!\}. \tag{7}$$

Note that oblique movements between adjacent cells are ignored in the present simulation. Lateral avalanching occurs under the same condition as in Eq. (5), but here, the slopes of interest are those in the positive and negative y-directions, which are defined as

$$\{\text{downward slope}\} = h(i,j) - h(i,j+1),\;\; h(i,j) - h(i,j-1), \tag{8}$$

respectively. If the lateral slopes in both the positive and negative y-directions are steeper than the angle of repose, only one of these two directions is selected, and they have equal probability:

$$A_{l+} = A_{l-} = \frac{1}{2}, \tag{9}$$

where A_{l+} and A_{l-} are the probabilities of avalanching in the positive and negative y-direction, respectively. In previous CA models for aeolian dunes, avalanching sand moves in the steepest direction (e.g., Werner 1995). In the present model, for simplicity, we adopted the assumption stated in Eq. (9). When averaged over time, this rule is equivalent to the distribution due to avalanching of sand in a sandpile (e.g., Bak et al. 1987); that is, the sand is distributed equally in all possible directions.

Simulation

The simulation in the present study was executed as follows. At each time step, the movement of sand slabs in the x-direction, due to both bedload transport and avalanching, was determined for each cell and updated in

parallel. Next, lateral avalanching (in the y-direction) was determined for each cell and updated in parallel. During a single step, avalanching occurred only once per cell (i.e., it was not repeated until perfect relaxation). This was done for simplicity and because we consider bedload transport, and thus, it is not necessary to obtain a static slope (in a strict sense) after perfect relaxation.

In selecting values for the phenomenological parameters, we made the following assumptions. The topographic height was taken to be the number of sand slabs, and therefore, β and A_r were positive integers. Because the slope of a stoss side of a bedform is always gentler than the corresponding lee slope, the inequality $1 < \beta$ should be satisfied. In addition, we impose the inequality $\alpha > \gamma(\beta - 1)$ because the migration of grains is faster on a stoss side than it is on the corresponding lee slope (see Eq. (2) for the gentlest lee slope). The value of α is selected arbitrarily, subject to the condition that it be sufficiently smaller than unity; this probability is as a surrogate for the velocity of sand particles. The simulation results are insensitive to α, apart from the rate of development for a given time step. For a given value of α, the values of γ should be sufficiently small that the above inequalities are satisfied; otherwise, the model will not adequately reproduce the shielding effect of lee slopes. For simplicity and to take account of the above inequalities, we used the following values for the parameters: $\alpha = 0.05$, $\beta = 2$, $\gamma = \alpha/8 (= 6.25 \times 10^{-3})$, and $A_r = 4$. We let $q_b = 1$, which represents the assumption that the bedload is a thin layer. We let $q_a = 2$ so that there was a fast relaxation of the avalanching; however, we note that when $q_b = 1$, the simulation results were very similar, providing α was sufficiently smaller than unity. The initial state of the bed was almost flat, with some small random variation, for the available sediment (sand slabs), while the substrate was perfectly flat. The calculation space was a 200×40 grid of cells, although we also used a 400×80 grid of cells to make particular comparisons. Calculation runs were performed for more than 10^5 time steps, using a periodic boundary condition. Because the simulation was a minimal model and used the simplest formulae and boundary condition, the main discussion will be restricted to the case of sparse available sediments. We note that when sediments are plentiful, the interference between opposing boundaries cannot be ignored, and thus, it is not appropriate to use a periodic boundary condition.

Results and discussion

Development of sand topographic features

First, to evaluate the present model, we qualitatively assessed the dependence of the topographic features on the amount of sand, as expressed by the average sand thickness, which is defined as the total number of sand slabs divided by the number of cells in the system. In our simulation, the following types of bed appeared (in order of increasing amount of sand): sheet flows, sand patches, isolated (barchan) ripples, and continuous ripples. When the average sand thickness was less than 0.6, bedforms (ripples) were not generated, and sand migrated only as a veneer of fast-moving sand particles, which is referred to as sheet flow (Bagnold 1941; Cooke et al. 1993; Venditti et al. 2005). When the average sand thickness was about 0.65 (0.6–0.7), sand patches (small bunches of sand; Bagnold 1941; Cooke et al. 1993) appeared and coexisted with sheet flows, but no stable ripples occurred. Sand patches were repeatedly generated and destroyed, returning entirely to sheet flows (Fig. 1). Such a situation is commonly seen in flume experiments, and this contrasted to the case of ripples, which, once formed, were robust and maintained their shape during migration. Ripples were generated only when the average sand thickness was greater than 0.7. When the average sand thickness was less than 22, the ripples were barchans, an isolated type of ripple that typically takes a crescent shape (Fig. 2a); this is consistent with the

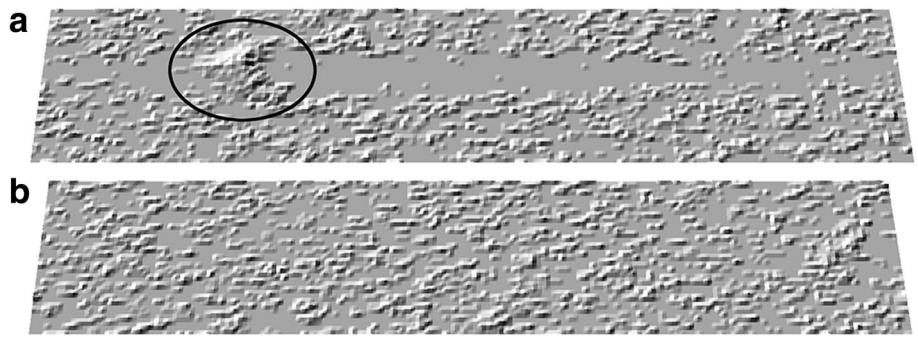

Fig. 1 Sand patches repeatedly appearing and disappearing. An identical run (average sand thickness of 0.65) is shown at different times: **a** 35,000 steps, **b** 50,000 steps; the sand moves from the left to right. A sand patch (enclosed by the *oval* in **a**) vanished 15,000 steps later. Note that there is only a little sand in the area downstream of the sand patch, which suggests that the sand patch gathers sand from upstream. Nevertheless, under this condition, the sand patch does not grow to an isolated ripple. The height of one slab is one-tenth the length of one cell

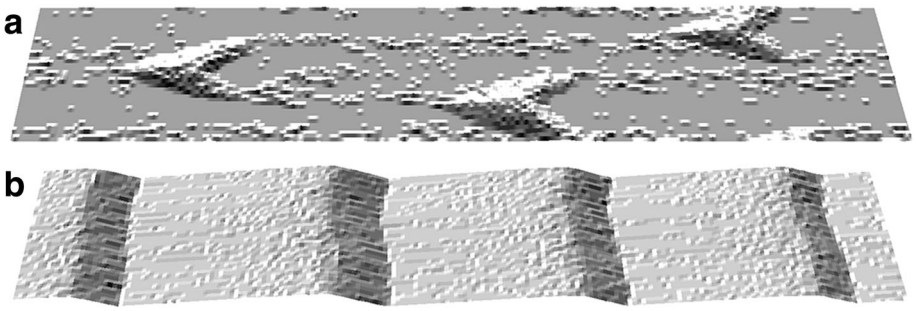

Fig. 2 Calculated topographies from the oblique view. **a** Isolated ripples (barchan ripples) and **b** continuous ripples; shown for the same time (10^5 steps), with average sand thicknesses of 1.0 and 30, respectively. The movement of particles is from the left to right, and in the graphics, the light is cast from the upper left. The height of one slab is one-tenth the length of one cell

finding that barchans form when the amount of sand is not sufficient to cover the entire area, as found by field studies (Bagnold 1941; Allen 1968; Wasson and Hyde 1983; Cooke et al. 1993) and flume experiments (Mantz 1992; Niño and Barahona 1997; Kleinhans et al. 2002; Endo et al. 2004, 2005; Dreano et al. 2010). As is well known, if there is abundant sand, a bed will have continuous ripples (e.g., Bagnold 1941; Allen 1968; Wasson and Hyde 1983; Dreano et al. 2010). In our simulation, when the average sand thickness was more than 22, continuous ripples were generated (Fig. 2b). Thus, the present simple model qualitatively reproduces the development of sand topographies that are due to the size of the bedload. Below, we will consider the starved state (beds with sparse sediments).

Temporal changes in sand flux compared with flume experiments

The sand flux is defined as the sand discharge per width (note that this differs from the general definition of flux in terms of the unit cross section). The sand discharge does not distinguish between that due to flow motions and that due to avalanching, and therefore, the sand flux includes both bedload transport and avalanching. If the sand discharge is quantified by bulk volume (including both sand and intergrain voids) per unit time, the dimensions of sand flux are the square of length over time (L^2/T), because the volume per width is measured in units of L^2.

It is known that when a bedform develops from a flat bed, the migration velocity decreases, but the size of the bedform increases asymptotically (Baas 1994; Coleman et al. 2003; Perillo et al. 2014). However, the actual time dependence of the sand flux has rarely been measured; this is probably due to the difficulty of doing so. As one example, Betat et al. (2002) used statistical methods to measure the sediment transport rate, the average height, and the migration velocity of irregular bed states during the development of bedforms. According to a graph presented in Betat et al. (2002), the sediment transport rate decreased monotonically with time, except at the very start of the experiment. Although this showed the temporal change in the sand flux, the definition of the sediment transport rate in that paper (Betat et al. 2002) was different from the usual definition of sand flux. For a comparison using the usual definition, the measured values were transformed to the sand flux using the simple relation $Q \propto H \times V$, where Q is the sand flux, H is the height of the bedform, and V is the migration speed. If the sand discharge is measured by bulk volume instead of weight, $Q = H \times V$ (Dreano et al. 2010). Although actual beds are irregular, especially during the development of bedforms (before reaching equilibrium), this relation can be applied to the data of Betat et al. (2002), because these are spatial averages for each moment and are obtained through precise measurements and calculations; therefore, they are suitable for estimating the overall trend of the sand flux.

Figure 3 shows the temporal changes in the reconstructed sand flux and the bedform developments found in experiments (Betat et al. 2002). The sand flux decreased monotonically as it transitioned from a flat bed to a stable state; however, note that such a decrease in the sand flux is not generally observed, because natural locations are generally regarded to be in a stable state relative to the time scale of the observation. There has been little discussion of the decrease in sand flux prior to a stable state that is seen in mathematical models.

Figure 4 shows an example of the temporal changes in sand flux, as seen in the present model; note that the flux is spatially averaged over momentary values, and the standard deviation of the topographic height is used as an index of bed development. The simulation showed that the flux decreased monotonically as the bedform developed and enlarged. This change qualitatively agrees with the results of the experiment (Fig. 3), which had not been explicitly reproduced in previous models.

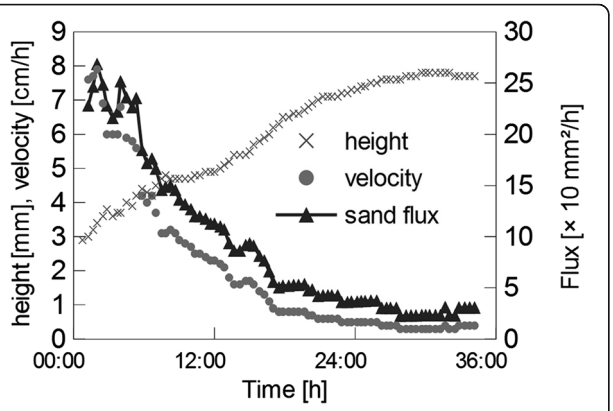

Fig. 3 Experiment: temporal development of velocity, height, and reconstructed sand flux of aqueous bedforms. The original data are taken from Betat et al. (2002). The sand flux is calculated using Bagnold's relation with a constant of unity, velocity × height, to show the relative change

Calculated sand flux in a stable state and its dependence on the amount of sand

In Fig. 5, the long-term stable state of the sand flux, as shown in Fig. 4, is compared to the average sand thickness (up to 3.5). For the range of average sand thicknesses shown in Fig. 5, the bed state changes from sand sheets through sand patches to isolated (barchan) ripples. Figure 5 shows that the sand flux increases and then decreases as the average sand thickness increases. The stage of increasing flux seems to directly reflect an increase in the amount of sand in the system, which likely corresponds to the supply-limited transport mode. The stage of decreasing flux in Fig. 5, however, cannot be explained by a supply limitation nor by a capacity limitation, because the model in this study does not explicitly calculate the fluid motion or the capacity of sediment transport due to flow. Additionally, the range of average sand thickness considered here (0–3.5) is a supply limitation in the ordinary sense of geomorphology and sedimentology, because the amount of sand is not sufficient to cover the entire substrate.

Figure 5 shows that the sand flux in a stable state increases and then decreases as the average sand thickness increases and the bed state changes from sand sheet through sand patches to isolated ripples. Additionally, in the cases in which we quadrupled the grid (400×80 cells), the total trend was identical, although the position and the value of the peak (ca. 5.5×10^{-1} and 8.6×10^{-3}, respectively) were slightly different (ca. 0.5×10^{-1} and 0.4×10^{-3} smaller, respectively). In the present model, Eq. (2), especially in the case of s2, indicates that the movement of a sand slab is suppressed by the topographic state of the adjacent downstream cell. In a specific test case in which condition (s2) was not included (sand migrates with constant probability regardless of the slope), the bedforms that formed did not have a plausible shape (stoss sides were steeper than lee slopes). This indicates the importance of interference by nearby particles in the development of beds; note that this works negatively in terms of sand flux.

Comparison with traffic flow and implications

As stated in the previous section, interaction between sand in neighboring cells (Eq. (2)) is necessary to reproduce bedforms with plausible shapes. Dynamic interaction between grains is a theme of physics of multiparticle systems or granular dynamics, and it is generally complicated. For specific topics, however, simplified models based on granular dynamics can reproduce real phenomena; an example of this is traffic flow. Although the

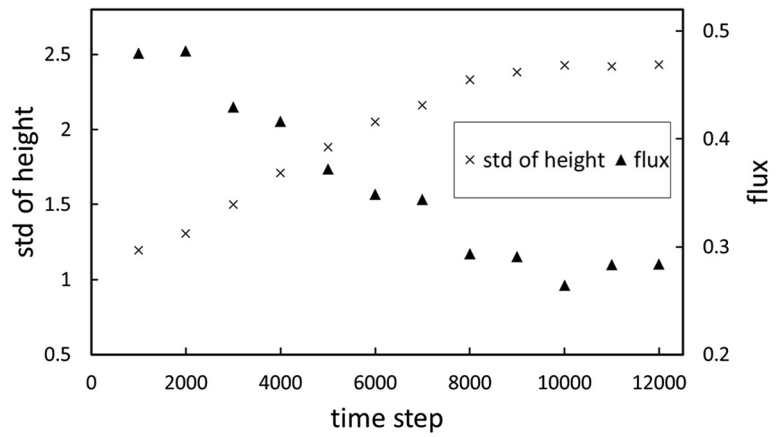

Fig. 4 Temporal change of sand flux and standard deviation (std) of the topographic height. The standard deviation of height is an index of the development of the bed, which increases as ripples enlarge; it can be easily calculated for irregular beds and isolated bedforms. Average sand thickness is 1.0. The height of the sand is equal to the number of sand slabs in each cell

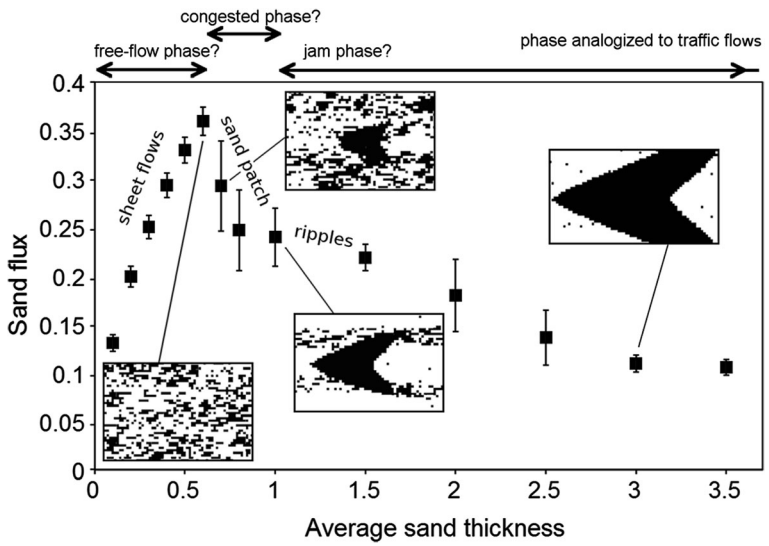

Fig. 5 Simulation: long-term sand flux against the average sand thickness. As shown in Fig. 4, the sand flux asymptotically decreases until the time step is approximately 10^4, and then it becomes almost constant with only a small fluctuation. The *bars* indicate the standard deviation of the fluctuation (the length of each bar is 2σ), which is obtained from data sampled every 500 steps from 1×10^5 to 5×10^5 steps for 10 runs under the same conditions (except for small random differences in the initially almost flat bed). The sand thickness is equal to the number of compiled slabs. The sand flux is the number of transported sand slabs per unit width per unit time step

present model for starved beds is built phenomenologically on the basis of the continuous bed-contact load, it has similarities to a model for traffic flows. Traffic flow is of interest both in the fields of physics and in civil engineering, where cars are regarded as grains and their flow considered a type of granular flow (e.g., Chowdhury et al. 2000). In such studies, the relation between car-flow phases (i.e., "grain-flow phases") and the abundance of cars (density of grains) has been investigated. The grain-flow phase is a class or state of transportation in a traffic flow, and the traffic viewpoint is different from the transport modes of geomorphology and sedimentology (such as rolling, sliding, saltation, and suspension). Previous studies of traffic flow have shown that car-flow phases are connected with car transportation rates (Chowdhury et al. 2000). Car transportation rates correspond to sand flux for sediment beds, which is a quantifiable factor. In geomorphology and sedimentology, while interconnectional properties among different levels of interaction (for example, grain–fluid, bedform–fluid, and bedform–bedform) have been identified (e.g., Kocurek et al. 2010), differences in the grain-flow phase have not been clearly identified. Here, we review a previous model of traffic flow and compare it with the present model in order to understand the relation between sand flux and the state of sand transportation on starved beds.

The stochastic optimal velocity (SOV) model (Kanai et al. 2005) is a stochastic CA model of the traffic flow. The simple SOV model considers the case in which a particle (car) migrates at most one cell per step, as in the present model for bedload transport. Before discussing the similarities between the present model and the SOV model, we will consider the difference. The simplest SOV model assumes a single-lane road and prohibits overtaking, whereas the present model for bedload transport allows overtaking. The present model accepts more than one particle (slab) per cell, which represents a compilation of sand, while the SOV model allows only one particle per cell.

A flux–density diagram is used to show the dynamic properties of car traffic flows. Because the average sand thickness in the present study is equivalent to the density of particles (the number of particles per unit area), Fig. 5 can be compared to a flux–density diagram of traffic flow. Despite the different research targets, the two models have common points. In both models, the probability of migration of particles corresponds to the velocity. The SOV model reproduces the relation between the flux and the density of particles, and it is asymmetric (fast increase and long-tailed decrease). This agrees with observations of a real highway (Sugiyama et al. 2008) and resembles the results of the present model (Fig. 5), although car traffic jams always propagate upstream. Interestingly, the curve in Fig. 5 shows an abrupt decrease around the peak before a tail. A similar abrupt decrease is seen in observations of real traffic and is interpreted as an overshoot of the free phase against the jam phase, showing a metastability bifurcation (Kanai et al. 2005).

When comparing the model of the present study and that of Kanai et al. (2005), we note that the stage of

increasing sand flux (average sand thickness of less than 0.6; sheet flows occur; Fig. 5) corresponds to the free-flow phase of traffic flows. The concepts of supply-limited sediment transport and free-flow phase are in accordance, in that they are free from interference from other particles. The state of decreasing sand flux (average sand thickness over 0.7; isolated ripples are generated; Fig. 5) corresponds to the jam phase. The vicinity of the peak sand flux (average sand thickness 0.6–0.7; sand patches repeatedly appear and disappear, while sand sheets exist continuously; Fig. 5) is the transition between the above two phases and likely corresponds to the congested phase. Therefore, it is suggested that sand topographic features on starved beds are dominated by the interference between sand particles.

Limitations of the present model and future developments for potential applications

It is important to note that the present minimal model can be applied only to specific cases in which the bedload transport rate is very low. For wider application, formulae should include other processes, such as erosional effects occurring downstream of lee slopes, three-dimensional effects of flows, and a more realistic avalanching process. These effects become important when bedform heights are large; therefore, the use of the present minimal model requires restricting the size of the bedload and bedforms.

It is interesting to consider a flume experiment that was conducted under conditions similar to those discussed above. Dreano et al. (2010) showed that in the stable state, the bedload flux due to bedform migration increased from barchan ripples to transverse barchanoid ripples if the sand supply was increased (however, we note that the setup of these experiments was different from the present simulation). Dreano et al. (2010) observed dynamic equilibrium states in which there was a well-controlled forced influx of sand into the system, while the present simulation assumes a closed system. In our simulation, we did not observe development of isolated ripples as the abundance of sand increased; instead, we investigated the relation between sand flux and the transition between sand sheets, sand patches, and isolated ripples, which had not been investigated sufficiently, compared with the properties of bedforms (ripples and dunes). In the personal experience of the author, during preliminary runs and at early stages of actual runs of flume experiments for different purposes, it is often observed that sand patches occur with thin sand sheets under conditions of sparsely available sediments. The sand patches migrate more slowly than do sand sheets, and this probably decreases the sand flux, although no measurements have been conducted (note that precise measurement of this is difficult). During the growth of sand patches, sand particles transported from upstream are incorporated into sand patches and decelerated (like cars on a congested road); this local state is not in equilibrium, but in a stochastic (statistical) sense, it does not violate the equilibrium of the entire system, because sand patches repeatedly appear and disappear in many places. Such behavior is compatible with the stochastic model. Although, the dynamics in the background of the stochastic process and the connection of the numerical model to actual beds remain to be further explored in future studies using new techniques for measurement and observation, considering the change in sand flux due to bed states through a grain-flow phase is a viewpoint that leads to a deeper understanding of bedforms and other sand topographies.

There have been jam-like phenomena reported, although those are more complicated than the present model. When sediments pass a meander bend of a river channel with a pool, the migration speed of sediments decreases greatly as they enter the pool, and it then increases as they leave (Kleinhans et al. 2002); this resembles the behavior of cars entering and leaving traffic jams. Another example is the pulsatory migration of bimodal mixtures of grain-sized sediment. A mixture of large grains (gravel) and finer grains repeats the clustering and scattering behavior when they are transported downstream as a bedload (Iseya and Ikeda 1987). It is considered that this behavior comes directly from the interference caused by the presence of other grains (i.e., jams), rather than from the water flow due to a moving boundary condition that is induced by the other grains. Such a situation is very complicated in the sense of the physics of multiparticle systems, but it could be at least partially explained by modeling it as a jam of transported particles; however, it would be necessary to add some new ideas to the present model.

Partially alluvial covers in bedrock river channels play an important role in the incision rate. Those can either promote incision by providing tools or inhibit incision by acting as armor. Finnegan et al. (2007) performed flume experiments with a straight channel and homogeneous sediments; they demonstrated that following sediment supply perturbations, the growth of roughness of the bedrock, which is caused by the deposition of alluvial cover, resulted in both negative and positive feedback to the average incision rate. Gravel in a channel, which can act as armor, can help preserve potential topographies; for example, inverted paleochannels on the floor of Miyamoto crater (Mars) were able to resist later (modern) aeolian erosion, as compared to the area outside the channel (Newsom et al. 2010).

When a bedrock channel is considerably rough, sparsely distributed sediments move in complicated ways. There is a need for a numerical model that can predict, for any shape of channel, the spatial and temporal variation of the

incision rates induced by sediment supply perturbations; beyond that, there is a need for a model that can do this for bimodal sediments. Although the present study considered only flat, nonerodible substrates, it may be possible to adapt it so that it can incorporate changes in roughness of the substrate; this could be done by formulating phenomenological equations for erosion due to partial alluvial covers.

Conclusions

A simple CA model simulating continuous bed-contact loads (rolling and sliding) is proposed; this model was developed phenomenologically and without the calculation of fluid motion. It is intended primarily for starved beds in a subaqueous system. As the amount of sand increases, the model reproduces the following bed types in order: sheet flows, sand patches, and ripples. While sand patches coexist with sand sheets and are not sustainable, ripples are robust once formed.

In the simulation, during bed development, the sand flux showed a monotonic decrease. This is in qualitative agreement with data from a previous well-controlled flume experiment that had not previously been reproduced by a numerical model.

In the stable state, the sand flux versus average sand thickness (flux–density relation) shows a steep increase followed by a tailed decrease, which is similar to the pattern seen in car traffic. The similarities between sand beds and traffic flow suggest that the changes in sand flux due to the bed state and the interference between sediments are important factors in the generation of bedforms, especially for the transition between topographies on starved beds. In the simulation, the change in sand topographic features corresponds well to the flux–density diagram. Sand topographic features shift at the fluxes of the boundaries between segments of the curve in the diagram (Fig. 5), which suggests that sand sheets, sand patches, and sand ripples correspond to the traffic phases of free flow, congested, and jam, respectively, depending on the degree of interference between sand particles.

Abbreviations

$h(i, j)$: Topographic height at position (i, j); $B_{i,j}$: Probability of sand migration by bedload transport, depending on the state at position (i, j); q_b and q_a: Numbers of slabs migrating by bedload transport and by avalanching, respectively, during a single calculation step; S_c: Critical slope of stoss side; A_r: Positive constant representing the angle of repose; β: Critical value for the shadow zone; α and γ: Positive constants that are parameters for $B_{i,j}$; A_{l+} and A_{l-}: Probabilities of avalanching in the positive and negative y-directions, respectively, in the case where both directions are possible

Acknowledgements

Special thanks are extended to Prof. F. Masuda of Doshisha Univ. for many hours of helpful discussion. Additionally, I would like to thank Dr. A. Katsuki for advice on the early version of the manuscript.

Funding

This study was financially supported by JSPS KAKENHI Grant Number 25350424.

Authors' contributions

NE performed calculations and drafted the manuscript.

Competing interests

The author declares that he has no competing interests.

Received: 3 December 2015 Accepted: 18 August 2016
Published online: 26 September 2016

References

Allen JRL (1968) Current ripples: their relation to patterns of water and sedimentation motion. North-Holland, New York

Allen JRL (1982) Sediment structures: their character and physical basis, vol 1. Elsevier, Amsterdam

Andreotti B, Claudin P, Devauchelle O, Durán O, Fourrière A (2012) Bedforms in a turbulent stream: ripples, chevrons and antidunes. J Fluid Mech 690: 94–128

Baas JH (1994) A flume study on the development and equilibrium morphology of current ripples in very fine sand. Sedimentology 41:185–209

Bagnold RA (1941) The physics of blown sand and desert dunes. Methuen, London

Bak P, Tang C, Wiesenfeld K (1987) Self-organized criticality: an explanation of the 1/f noise. Phys Rev Lett 59:381–384

Barchyn TE, Hugenholtz CH (2012) A new tool for modeling dune field evolution based on an accessible, GUI version of the Werner dune model. Geomorphology 138:415–419

Barrio-Parra F, Rodríguez-Santalla I (2014) A free cellular model of dune dynamics: application to El Fangar spit dune system (Ebro Delta, Spain). Comput Geosci 62:187–197

Betat A, Kruelle C, Frette V, Rehberg I (2002) Long-time behavior of sand ripples induced by water shear flow. Eur Phys J E: Soft Matter Biol Phys 8:465–476

Bridge JS, Demicco R (2008) Earth surface processes, landforms and sediment deposits. Cambridge University Press, Cambridge

Chowdhury D, Santen L, Schadschneider A (2000) Statistical physics of vehicular traffic and some related systems. Phys Rep 329:199–329

Coleman SE, Fedele JJ, Garcıa MH (2003) Closed conduit bed-form initiation and development. J Hydraul Eng 129:956–965

Cooke RU, Warren A, Goudie AS (1993) Desert geomorphology. Taylor & Francis, London

Diniega S, Glasner K, Byrne S (2010) Long-time evolution of models of aeolian sand dune fields: influence of dune formation and collision. Geomorphology 121:55–68

Dreano J, Valance A, Lague D, Cassar C (2010) Experimental study on transient and steady-state dynamics of bedforms in supply limited configuration. Earth Surf Proc Land 35:1730–1743

Duran O, Claudin P, Andreotti B (2014) Direct numerical simulations of aeolian sand ripples. Proc Natl Acad Sci U S A 111:15665–15668

Endo N, Taniguchi K, Katsuki A (2004) Observation of the whole process of interaction between barchans by flume experiments. Geophys Res Lett 31:L12503

Endo N, Sunamura T, Takimoto H (2005) Barchan ripples under unidirectional water flows in the laboratory: formation and planar morphology. Earth Surf Proc Land 30:1675–1682

Finnegan NJ, Sklar LS, Fuller TK (2007) Interplay of sediment supply, river incision, and channel morphology revealed by the transient evolution of an experimental bedrock channel. J Geophys Res 112:F03S11

Iseya F, Ikeda H (1987) Pulsations in bedload transport rates induced by a longitudinal sediment sorting: a flume study using sand and gravel mixtures. Geogr Ann A 69:15–27

Kanai M, Nishinari K, Tokihiro T (2005) Stochastic optimal velocity model and its long-lived metastability. Phys Rev E 72:035102

Katsuki A, Kikuchi M, Endo N (2005) Emergence of a barchan belt in a unidirectional flow: experiment and numerical simulation. J Phys Soc Jpn 74:878–881

Kleinhans MG, Wilbers AWE, De Swaaf A, Van Den Berg JH (2002) Sediment supply-limited bedforms in sand–gravel bed rivers. J Sediment Res 72: 629–640

Kocurek G, Ewing RC, Mohrig D (2010) How do bedform patterns arise? New views on the role of bedform interactions within a set of boundary conditions. Earth Surf Proc Land 35:51–63

Mantz PA (1992) Cohesionless, fine-sediment bed forms in shallow flows. J Hydraul Eng 118:743–764
Melo HP, Parteli EJ, Andrade JS, Herrmann HJ (2012) Linear stability analysis of transverse dunes. Physica A 391:4606–4614
Miyata Y, Iwasa S (1997) Ripple initiation by random grain-rolling: water-tank experiment and numerical simulation. In: Abstracts of the 104th annual meeting of the ecological society of Japan., p 319
Momiji H, Carretero-Gonzalez R, Bishop SR, Warren A (2000) Simulation of the effect of wind speedup in the formation of transverse dune fields. Earth Surf Proc Land 25:905–918
Newsom HE, Lanza NL, Ollila AM, Wiseman SM, Roush TL, Marzo AG, Tornabene LL, Okubo CH, Osterloo MM, Hamilton VE, Crumpler LS (2010) Inverted channel deposits on the floor of Miyamoto crater, Mars. Icarus 205:64–72
Niiya H, Awazu A, Nishimori H (2010) Three-dimensional dune skeleton model as a coupled dynamical system of two-dimensional cross sections. J Phys Soc Jpn 79:063002
Niño YB, Barahona M (1997) Barchan-ripples: emergence, evolution and flow–sediment interactions. Proc Int Assoc Hydraul Res 27B:1037–1042
Nishimori H, Ouchi N (1993) Formation of ripple patterns and dunes by wind-blown sand. Phys Rev Lett 71:197
Parteli EJR, Herrmann HJ (2003) A simple model for a transverse dune field. Physica A 327:554–562
Perillo MM, Best JL, Yokokawa M, Sekiguchi T, Takagawa T, Garcia MH (2014) A unified model for bedform development and equilibrium under unidirectional, oscillatory and combined-flows. Sedimentology 61:2063–2085
Reid I, Frostick LE (1994) Fluvial sediment transport and deposition. In: Pye K (ed) Sediment transport and depositional processes. Blackwell Scientific, Oxford, pp 89–155
Rozier O, Narteau C (2014) A real-space cellular automaton laboratory. Earth Surf Proc Land 39:98–109
Schwämmle V, Herrmann HJ (2003) Geomorphology: solitary wave behaviour of sand dunes: colliding dunes appear to traverse through one another and emerge unscathed. Nature 426:619–620
Sugiyama Y, Fukui M, Kikuchi M, Hasebe K, Nakayama A, Nishinari K, Tadaki S, Yukawa S (2008) Traffic jams without bottlenecks: experimental evidence for the physical mechanism of the formation of a jam. New J Phys 10:033001
Venditti JG, Church M, Bennett SJ (2005) Morphodynamics of small-scale superimposed sand waves over migrating dune bed forms. Water Resour Res 41:W10423
Wasson R, Hyde R (1983) Factors determining desert dune type. Nature 304:337–339
Werner B (1995) Eolian dunes: computer simulations and attractor interpretation. Geology 23:1107–1110
Werner BT, Kocurek G (1999) Bedform spacing from defect dynamics. Geology 27:727–730
Wippermann F, Gross G (1986) The wind-induced shaping and migration of an isolated dune: a numerical experiment. Bound-Lay Meteorol 36:319–334